

# A Fast Shaping Low Power Amplifier-Comparator Integrated Circuit For Silicon Strip Detectors\*

Edwin Spencer, David Dorfan, Alex Grillo, Sergei Kashigin, William Rowe, Alec Webster, and Max Wilder

SCIPP, University of California, Santa Cruz, CA 95064



## Abstract

We have designed and tested a 64 channel amplifier-comparator integrated circuit on the Maxim SHPi bipolar process. The low power design, 840  $\mu$ W/channel, is intended for use as a front-end with high clock rate silicon strip detector systems. Peaking time at the comparator input is 20 ns, for good double pulse resolution, and noise is near optimum for the technology used. We have used the chip successfully in a proton beam test at KEK in Japan with a 40 MHz data clock.

## I. INTRODUCTION

Silicon strip detectors used as vertex detectors in high rate colliders are well suited for integration with multichannel integrated circuit amplifiers[1]. Inclusion on the IC channel of a single precision comparator with a digital output provides a low power and low cost front-end analog system, yet provides capability to measure system characteristics such as noise, crosstalk and efficiency. We developed the LBIC IC as a prototype amplifier-comparator for the SSC silicon tracker, so it has direct applicability for binary readout of the trackers proposed at LHC. In this paper, we will review the general specifications of the frontend system, then describe the circuit details, and discuss chip test results, which will include effects of proton irradiation on the LBIC.

## II. SPECIFICATION

**Amplifier peaking time:** The channel digital output needs to be assigned to the correct collider bunch crossing, which occurred every 16 ns in the SSC. Silicon strip signals in 300  $\mu$ m thick detectors can take up to 25 ns to collect. For good signal/noise, shaping time should be longer than collection time. A comparator with fixed threshold will fire earlier on a larger amplitude signal for a given signal shape. Comparator firing time variance on the range of signal amplitudes, called time walk, should ideally be at least 5 ns less than the bunch crossing rate in order to allow easy

assignment to a unique time bucket. Time walk for a signal shape is mostly dependent on the signal peaking time. In our design, the comparator itself contributes less than 1 ns of time walk on all amplitudes of signals. We want to keep double pulse resolution to 60 ns or less, which in practice implies a peaking time of at most 20 ns. Balancing these considerations, we selected a 20 ns peaking time. For the SSC this might have necessitated time walk correction circuitry, which the LBIC design does not include. For the LHC, which has beam crossings of 25 ns, a time walk requirement of 20 ns is a good match for the LBIC shaping.

**Chip power use:** At a hadron collider the silicon tracker is deep inside a massive 4 $\pi$  detector. Heat from circuit power use must be removed, and material used in transporting the heat out of the detector increases the interaction probability for particles. Power use for this chip was specified to be below 1mW/channel, with any further reduction being useful.

**Noise:** Silicon strip signals in 300  $\mu$ m detectors are small: the most probable amplitude is about 4 fC. Setting the discriminator threshold at 1 fC has been shown in beam tests to give good efficiency. To keep the noise false hits at a low rate, we need to set the threshold at the 4 sigma level of the strip channel noise. In addition to simple bipolar amplifier noise, there is series noise from the detector strip resistance, shot noise from irradiated detector leakage current, and noise from adjacent strips. Neighboring strips are important since strip capacitive load is mostly with its neighbors. Since the shaping time is similar to the signal itself, there is also some ballistic deficit, typically about 10 %. A 12 cm long n-type detector strip presents an 18 pF capacitive load, and typically has a noise of  $\sigma = 1600 e^-$  at 20 ns shaping, when we consider all noise sources. Ballistic deficit raises this to an equivalent 1800  $e^-$ . Four times this noise implies a threshold of 1.15 fC of n-type signal. We must optimize amplifier noise contributions, as well as the other noise

SCAN-9504015



sw9515

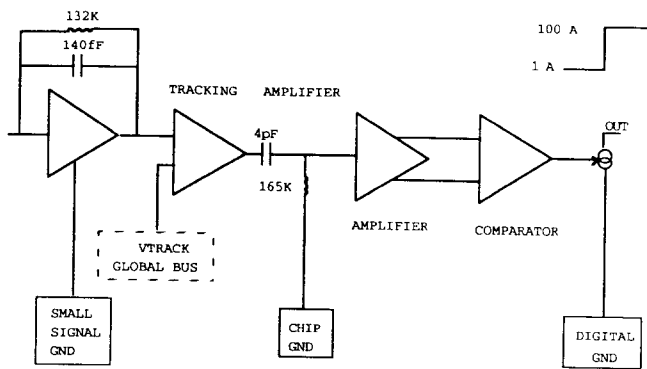


Figure 1. LBIC functional block diagram.

sources, to keep the particle detection efficiency high.

**Precision:** All the channels on a chip get a common threshold at their comparator inputs, so the false hit rate will be dominated by the amplifier with the highest gain. An acceptable increase in false hit rate is found with an equivalent channel variation of one-third the noise, or equivalent threshold sigma of 0.08 fC of input signal.

**System pickup:** Sporadic digital pickup increases the apparent frontend noise, so it must be avoided. Synchronous digital clock pickup can cause offsets between channels, which reduces matching precision and introduces clock phase dependence of the effective threshold. The frontend system needs all the isolation from the digital readout that we can provide.

**Radiation Resistance:** SSC and LHC specified good performance for a fluence of at least  $2 \times 10^{14}$  protons/cm<sup>2</sup>. Channels in a given module using a common threshold are assumed to receive the same fluence. The main radiation effect is a decline in npn DC beta, initially about 100, to about 40, so the design must compensate for this change.

**Cost and mass:** Chip area needs to be minimized. The silicon chip mass is a substantial contributor to the material in the detector volume. Precision needs to be attained without adding the expense of laser trimming or special selection procedures. Minimizing chip area will minimize cost if yields can be kept high.

### III. DESIGN

We chose Maxim's SHPi process, which has 8 GHz  $f_t$  npn's with a minimum emitter size of  $1.3 \times 3.6 \mu\text{m}$ [2]. The very low npn

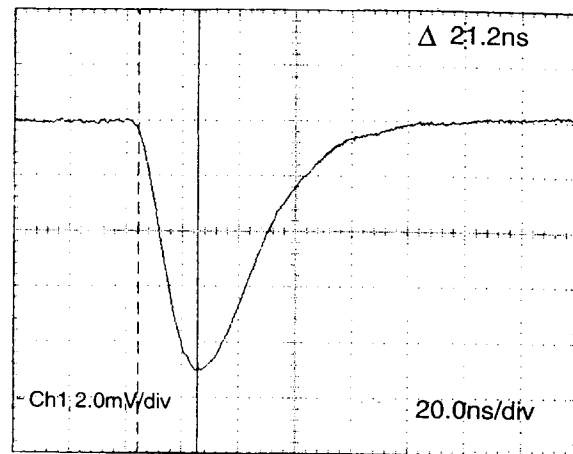


Figure 2. One of two signals at the differential comparator input.

collector capacitance enabled us to set quiescent biases as low as  $2.7 \mu\text{A}$  with correct design bandwidth, and the very small emitter volume demonstrates sufficient radiation resistance. Typical npn beta is 100, with  $3 \sigma V_{be}$  matching of 1mV for adjacent npn's. Adjacent  $3 \sigma$  resistor matching is 1% and process resistor variation is  $\pm 22\%$ . SHPi allows very low currents, has sufficient precision, and possesses workable radiation resistance.

Figure 1 shows the five LBIC circuit stages of preamp, tracking amplifier, AC coupling, amplifier, and comparator with open collector output. The tracking amplifier boosts the dynamic signal before the AC coupling, so that we minimize the threshold errors contributed by later stage DC variations. Gain is 180 mV/fC at the comparator input, determined by precision design concern. Analog signal shape, Figure 2, is semigaussian for fast return to the baseline, best for double pulse resolution. Three analog probe points are provided on even numbered channels, PR1 - PR3.

Figure 3 is the channel subcircuit, 64 on each chip. Figure 3 also indicates the global buses. The primary supplies are V3.5 and ground. Ground is supplied to 3 independent buses for stage isolation. The other chip supplies are the differential threshold, VT1 and VT2, and V7. VFRONT global bus provides current sink bias at  $3.3 \mu\text{A}$  per minimum transistor unit.

In the preamp, J1 is an active current source, whose gate is controlled by a global voltage bus, VJ1. This bus is driven by a simple op-amp circuit that needs a supplementary 7 V supply, V7. J1 current is programmable by an external voltage. 0 V sets J1 at  $130 \mu\text{A}$ , the noise minimum for 14 pF front load with an irradiated chip. Q1 input transistor is 8 times the minimum transistor size as a noise trade-off between declining

irradiation beta and base resistance of  $54 \Omega$ . Cascode Q2 increases preamp open loop gain which lowers the front input impedance, and decreases strip crosstalk. Capacitor feedback, C4 and C1, is split, which increases the gain of diff amp Q8-Q11 by lowering the dynamic emitter impedance of Q8. This saves power. Additionally, split feedback narrows the preamp bandpass, giving a semigaussian rather than RC-CR signal shape.

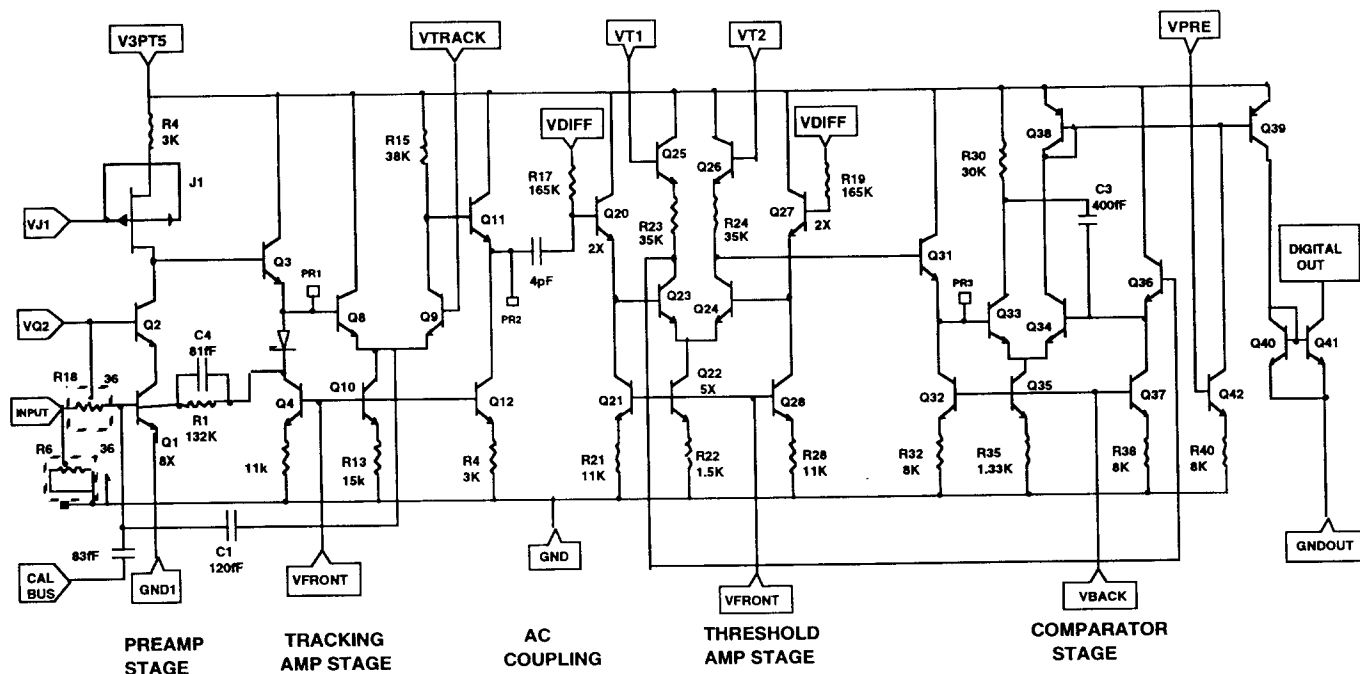
Under irradiation, the emitter of Q3 shifts 300 mV as Q1 base current goes from 1 to 3  $\mu\text{A}$ , since this current is supplied through feedback R1. The tracking amp stage, Q8 - Q11 has a global voltage bus, VTRACK, that tracks the preamp output and biases Q9 as a voltage source. A heavily decompensated preamp circuit, Figure 4, drives the VTRACK bus. Note that the circuit depends on cross chip component matching since more than 5 mV mismatch in VTRACK brings a noticeable gain change in the diff amp. The collector of Q9 is a signal integration point.

We make the AC coupling time constant as large as chip space allows. After this coupling, circuitry is full differential for DC precision. VDIFF global voltage, 2.2 V, provides DC input bias. The next diff amp has the differential thresholds, VT1 and VT2, applied to its collector voltages, where the full differential signal is integrated for the third time. The full differential threshold allows the threshold to be applied across many channels

and chips with good common mode rejection. The differential dynamic signal is applied to the comparator stage, Q31 - Q42.

The comparator current output is shown in Figure 5. A differential pair with AC positive feedback forms the comparator amplifier. VBACK global voltage biases current sinks at 4 mA per transistor unit emitter area. The comparator transfer function, Figure 6, shows a decreasing offset with increasing signal, with a small signal threshold offset of -29 mV. Offset is the difference between the expected comparator response of unity transfer and the actual response. The collector of Q33 only begins to swing when the signal approaches within about 50 mV of the diff pair balanced bias point. The top 50mV of a large signal has a lower slew rate than a smaller signal has for the same interval. Positive feedback decreases with slew rate, implying that with larger thresholds, a bigger offset of the diff pair, the dynamic signal approaches closer to the diff pair balanced bias point before the comparator switches.

When the comparator switches, the tail current of 24  $\mu\text{A}$  begins flowing through Q38 and appears as a 100  $\mu\text{A}$  digital signal into the Q41 collector, with a minimum width of 25 ns. Only about 5 mV of comparator input range gives an insufficient digital pulse width, narrower than 25 ns. Global bus VPRE and Q42 keep the output at 1  $\mu\text{A}$  for the off state.



All transistors 1x unless noted

Figure 3. LBIC channel schematic, 1 of 64.

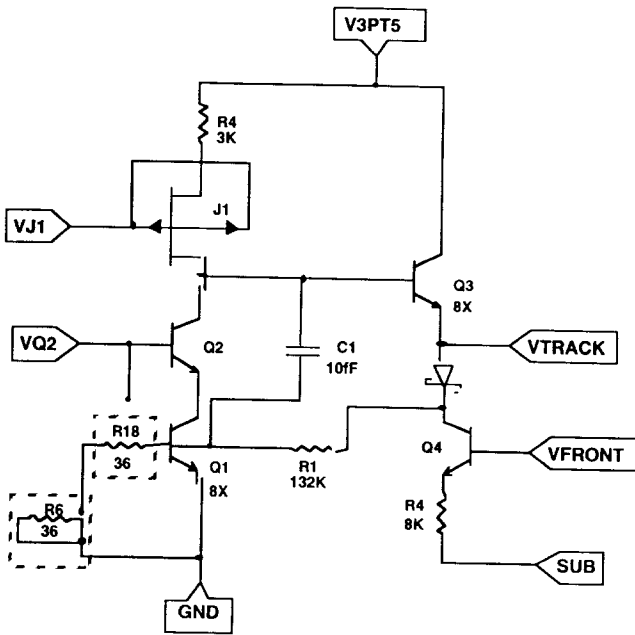


Figure 4. VTRACK global bus generator.

Layout of the LBIC channels is on a 40  $\mu\text{m}$  pitch, so that the chip matches a 50  $\mu\text{m}$  pitch strip detector. V3.5 has a 72 pF bypass cap. All the global voltage buses and supplies have a bypass capacitor of typically 7 pF to chip ground, except VTRACK. On the input of each channel is an 84 fF MIM calibration capacitor, the other end of which is tied to one of four calibration buses in alternating fashion.

#### IV. MEASUREMENTS

We measure the LBIC performance using a 64 channel input CMOS digital chip, the CDP, that we have fabricated in several versions: 1.2  $\mu\text{m}$  MOSIS, .8  $\mu\text{m}$  MOSIS, and .8  $\mu\text{m}$  Honeywell rad-hard[3]. The CMOS chip provides the digital reference ground, GNDOUT in Figure 3. The digital/analog isolation zone takes place on the LBIC itself between the high impedance collector of Q39, which is referenced to V3.5, and diode connected Q40, referenced to digital ground. The CDP receives the open collector LBIC signal with a diode connected PMOS transistor with an input impedance of 4 k $\Omega$ . This current is then compared with a programmable threshold, typically 40 % of full signal. We prototyped this LBIC only for p-strip signals, although it works with n-strips with a reversal of output levels. The n-strip output time widths are also narrower.

We constructed four assemblies each consisting of a Hamamatsu double-sided detector mounted on a pc board. 128 channels on each detector face were bonded to a total of 16 LBIC chips. We then developed a complete

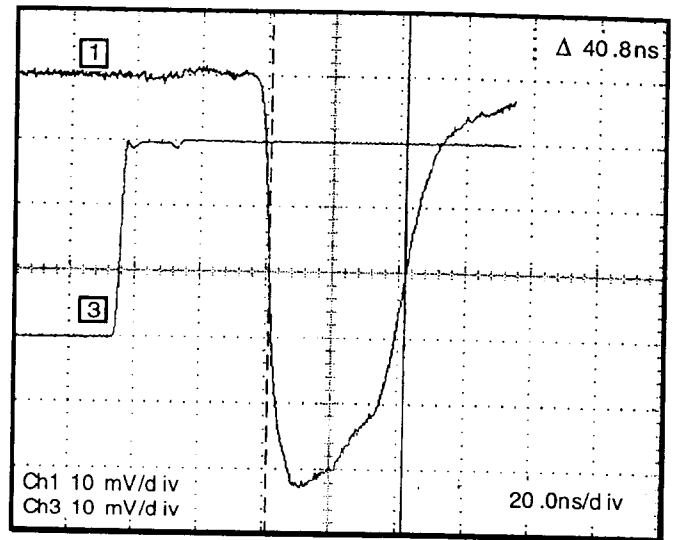


Figure 5. Digital output current signal into 600  $\Omega$ .

calibration and readout system at 40 MHz clock rate and tested this system in a beam test in June, 1994 at KEK. All measurements are done using this system. For channels bonded to a detector, digital clock pickup at 40 MHz is small. For channels that are unloaded, clock pickup can skew gain measurements, and we have to take some care.

We measure the response of a channel to a constant input charge by varying the threshold settings. At each threshold, we record the comparator hit percentage and create a plot as in Figure 7. The noise sigma is estimated by fitting a gaussian error function to the curve, since the noise has a white spectrum.

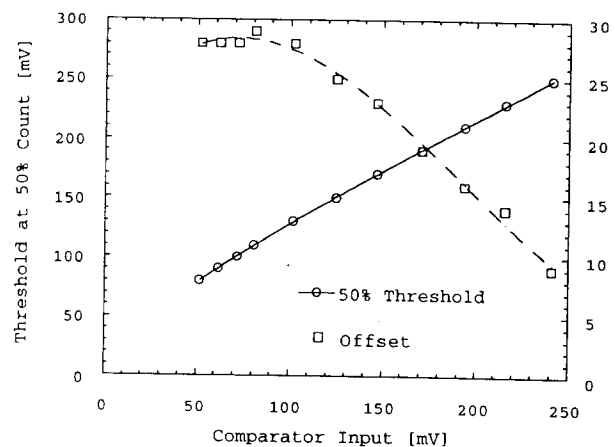


Figure 6. Comparator transfer function and offset versus single-ended signal injected into comparator by probe.

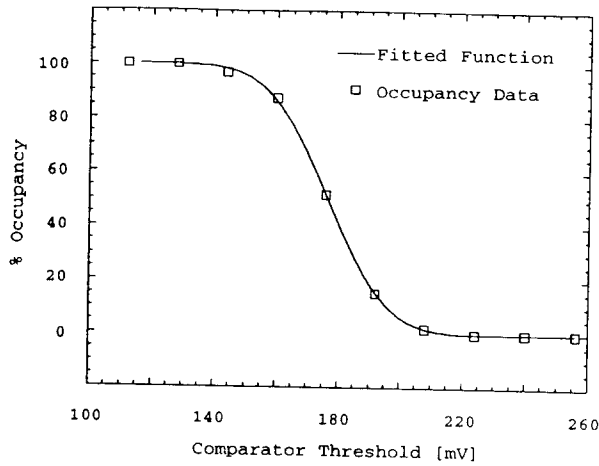


Figure 7. Count fraction versus comparator threshold.

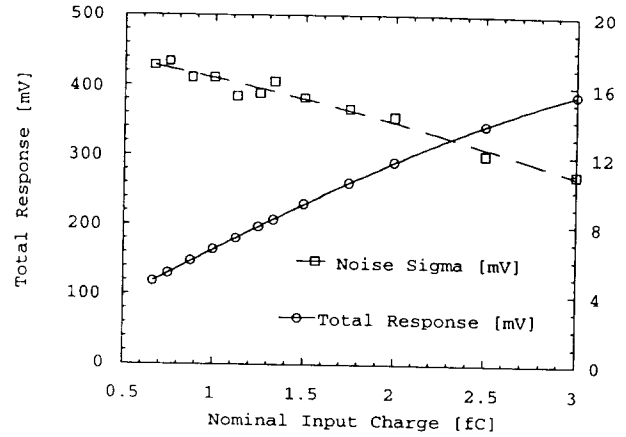


Figure 8. LBIC output response and measured noise versus input charge.

The 50% point defines the amplifier response.

Figure 8 shows the total response of the amplifier-comparator on a channel with no load, along with the derived output noise over a range of input charge. To determine amplifier gain and effective comparator offset from the response curve, we fit a cubic. The constant term in the cubic is taken as the effective comparator offset. Total gain is calculated from the remaining terms.

Input noise does not actually decrease with gain as the output noise in Figure 8 might indicate. Figure 9 shows the derivative of the total response, the small signal gain. The circuit amplifies a noise impulse by this small signal gain, since noise is usually a small

impulse riding on the hump of the calibration signal.

Figure 9 indicates that noise is a constant ratio to small signal gain. Using the 1 fC total gain, not the small signal gain, this unloaded channel shows 632 e- noise sigma. Total gain at 1 fC is typically 166 mV/fC.

Figure 10 shows noise versus capacitive load, which is a chip capacitor bonded to the input and the printed circuit board ground. Noise, at a 120  $\mu$ A front transistor bias, is 580 e- + (32 e-)/(pF), which is very close to simulations. The 9 pF data point shows lower noise than expected because the load capacitor, its inductive bonds, and the channel input form a resonant LCR circuit. The signal peaks more, which improves signal/noise. Detector strip loads do not show this resonant effect.

We compare channel to channel matching

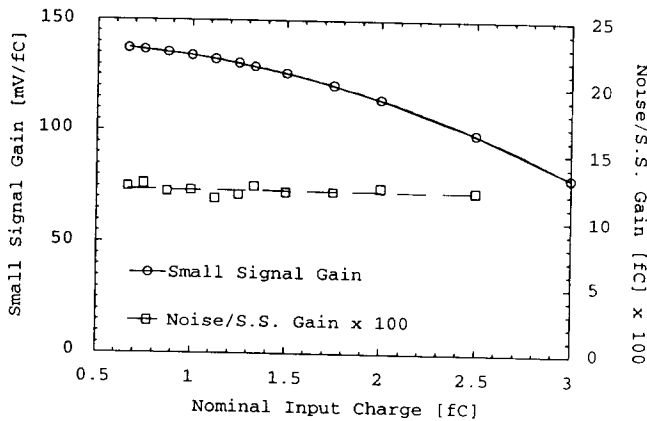


Figure 9. Small signal gain and (output noise)/(small signal gain) versus input charge.

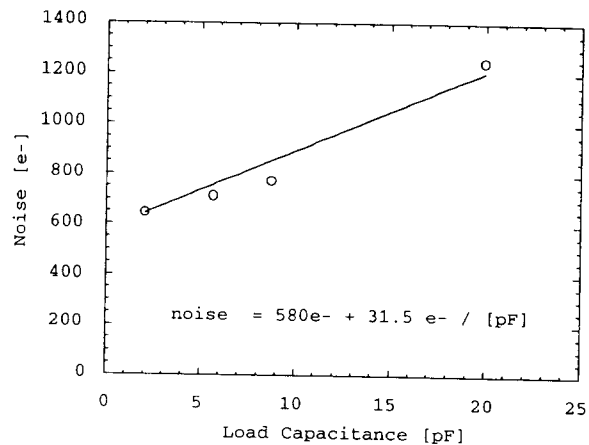


Figure 10. Noise versus capacitive load.

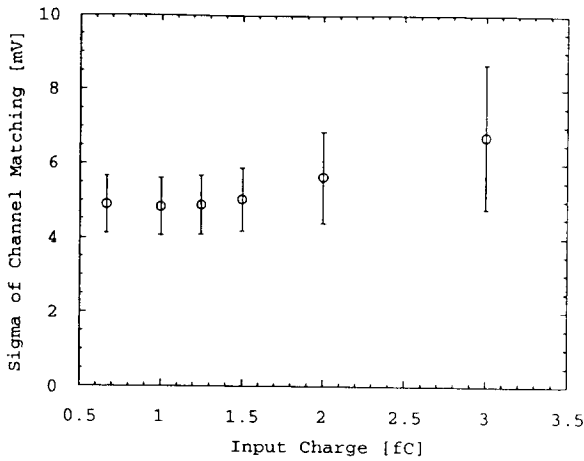


Figure 11. Channel to channel matching in mV for 3 chips as a function of input charge

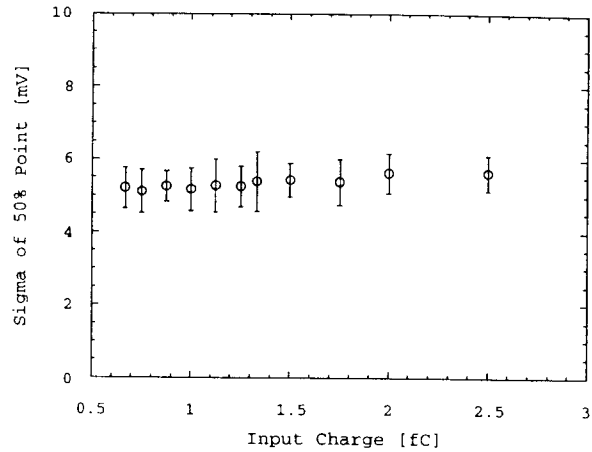


Figure 12. Channel to channel matching in mV for one chip after irradiation.

of input response within a chip for 3 chips. Figure 11 shows a sigma of 5 mV at 1 fC input, or 3 % variance of 1 fC gain. This includes calibration capacitor variation, channel gain variation, comparator offset differences, and any difference in digital pickup across the chip. From this measurement, we conclude that the global voltage sourcing technique works well.

Four LBIC and CDP chip sets were irradiated with  $5 \times 10^{13}$  protons/(cm)<sup>2</sup>. Figure 12 indicates that the channel matching for 59 channels on one chip remained very good,  $\sigma = 5.2$  mV. The lateral pnp beta declined to 4.5, which lowered the digital output to 64  $\mu$ A. Five channels had their comparator function shift in an unexpected way due to erratic pnp

deterioration.

Figure 13 indicates average input response for 4 chips: the 3 unirradiated from Figure 10, and the one irradiated from Figure 11. No significant change in response is seen for the irradiated chip. Matching chip to chip for this wafer is good enough to allow common thresholds without having to move thresholds higher in order to reduce noise hits.

The VTRACK bus had insufficient on-chip bypassing, and we found 1% channel to channel negative crosstalk on all chip channels. This is not a problem in actual use where simultaneous hits are rare, but 16 channels fire when calibrating, introducing 16 % low gain at 1 fC. Figure 14 shows the gain correction curve between single channel operation and 16 channel calibration. We placed a bypass capacitor to ground on the VTRACK bus by

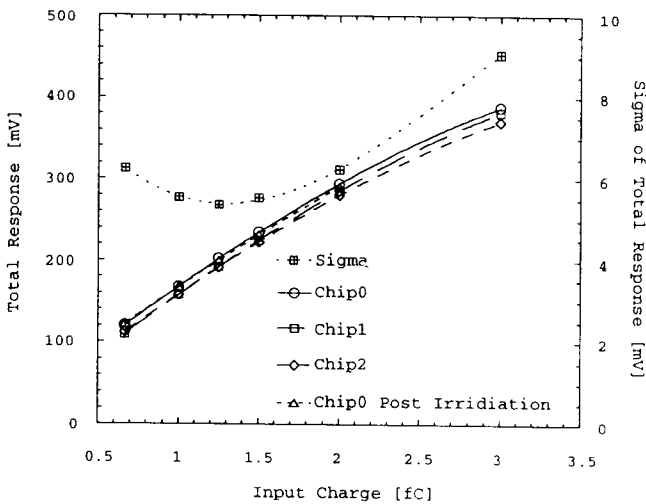


Figure 13. Four chip average response and variation of response over input.

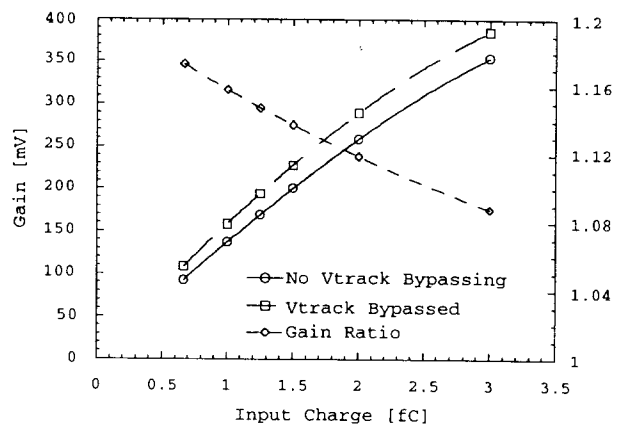


Figure 14. Response for VTRACK bypassed and not bypassed, and gain correction ratio.

using steel probes. The two response curves shown are with the bypass on and off the bus.

## V. CONCLUSION

The LBIC design meets the typical specifications needed for the LHC. The design meets specifications for the late SSC, except possibly for time walk. With very low power of .84 mW/channel, we have demonstrated precision amplifier/comparator functioning and matching. Noise is near optimum. Radiation resistance of the design is evident to  $5 \times 10^{13}/\text{cm}^2$  proton fluence. Lateral pnp's are not reliable at the fluences needed, but acceptable vertical pnp's are now available from Maxim. Digital pickup at 40 MHz has been shown to be negligible for channels with a detector load.

\* Work supported in part by U.S. Department of Energy and Texas National Research Laboratory Commission.

## VI. REFERENCES

- [1] E. Barberis, *et al.*, "A Fast Shaping Amplifier-Comparator Integrated Circuit for Silicon Strip Detectors", *IEEE Transactions on Nuclear Science*, Vol 40, No. 4, August 1993, pp. 740-743.
- [2] Maxim, Inc., formerly Tektronix, Inc., ICO, Beaverton, Oregon 97077.
- [3] Joel DeWitt, "A Pipeline and Bus Interface Chip for Silicon Strip Detector Read-Out", *Proc. of IEEE 1993 Nuclear Science Symposium*, San Francisco, CA, Nov. 1993.

